

# **Defect induced lowering of activation energies at step bands in Co/Cu(100).**

S.T. Coyle and M. R. Scheinfein

Dept. of Physics and Astronomy, PSF-470 Box 871504, Arizona State University, Tempe, AZ  
85287

James L. Blue

National Institute of Standards and Technology, Gaithersburg, MD 20899

## **Abstract**

Complex topological features such as rectangular voids and step inclusions that were seen in secondary electron micrographs of Co films grown on Cu(100) at room temperature were reproduced in Monte Carlo simulations in the presence of step bands. Lowered activation energies at defects such as steps, kinks, and vacancies enhance step edge restructuring during growth and upon annealing. This results in features such as faceted step edges, rectangular pits, incorporation of Co into terraces, surface alloying, and surface segregation. Simulated growth structures are directly compared with those observed in an ultrahigh vacuum scanning transmission electron microscope.

PACS: 68.35.Ct, 68.55.-a

**DTIC QUALITY INSPECTED 4**

### **DISTRIBUTION STATEMENT A**

Approved for public release;  
Distribution Unlimited

submitted APL

19971209 072

Experiments on the growth and magnetic properties of the Co/Cu(100) system often produce disparate results. STM studies of stepped Cu surfaces demonstrate that adatoms and kinks at steps are quite mobile.<sup>1,2</sup> Mobility at steps has also been studied theoretically using the embedded atom method.<sup>3,4</sup> It was suggested<sup>5</sup> that Fe islands which decorate step edges on Cu(111) relax the nearby Cu lattice, and decrease the activation energy for Cu diffusion along steps. This drives the migration of Cu and produces single-layer deep pits in Cu terraces. Large rectangular pits have been observed in Co/Cu(100) systems which have been annealed following room temperature (RT) growth.<sup>6,7</sup> These pits, from which Cu was believed to have migrated and covered the Co surface, typically formed near steps. An experimental study<sup>8</sup> of the growth and magnetic properties of Co/Cu(100) performed in our laboratory produced strikingly different growth morphologies under apparently identical conditions. Those observations were ascribed to two growth modes. The first growth mode is characterized by the formation of islands on terraces with little interaction with steps. The second growth mode is characterized by a lower island density and a high degree of interaction with and restructuring of step edges. A continuum of combinations of these two modes has been observed in different films. Kinetic Monte Carlo simulations have been performed for Co growth on Cu(100) in the presence of steps in an attempt to characterize these growth modes and the resulting film morphologies.<sup>9</sup> The first growth mode has been reproduced reasonably well. Enhanced roughening of step edges was observed in simulations, however, the length scale of features was smaller than the experimental results. The large scale etching features and pits characteristic of the second growth mode were not reproduced in the Monte Carlo simulations. This was attributed to the simple model of activation energies for processes at steps. Since the most striking morphological features

occurred near step bands, kinetic Monte Carlo growth simulations of Co on Cu(100) have been performed in order to characterize these unusual growth morphologies.

Simulations of the RT growth of Co on Cu(100) in the presence of step bands were performed. Prior to deposition the Cu substrate was discretized into a region 100 by 100 atoms square (along  $\langle 100 \rangle$ , 36x36 nm) and 14 layers deep (2.5 nm) with periodic boundary conditions. The region included one or two trenches with steps oriented along either  $\langle 100 \rangle$  or  $\langle 110 \rangle$ . The trenches, which were intended to simulate step bands, were 7 layers deep. The terrace width of each layer (step down) was four ( $\langle 100 \rangle$ ) or three ( $\langle 110 \rangle$ ) atomic rows. The simulations assumed an Arrhenius-type barrier model,<sup>10</sup> where the transition rate is  $r=R_0\exp(-\epsilon/kT)$ . Activation energies ( $\epsilon$ ) were set proportional to beginning and ending bond energies according to  $\epsilon = A/(1+|\Delta E|/B) + H(\Delta E)$ . The constant A is the energy barrier for hopping to a state of the same energy, and was set to approximate the experimental activation energy for Co adatom diffusion on Co(100).<sup>11</sup> H is the Heaviside function, T is the substrate temperature, k is Boltzmann's constant, and B is a constant which reduces the barrier somewhat when the initial and final energies differ. A and B were each set to 0.5 eV. The attempt frequency ( $R_0$ ) for the transition rate was  $2 k T/h$ , where h is Plank's constant. The Co-Co bond energy was 0.271 eV/nearest-neighbor (NN) and 0.004 eV/next-NN (NNN).<sup>12</sup> The Cu-Cu bond energy was 0.190 NN and 0.003 eV/NNN.<sup>12</sup> The Co-Cu bond energy was 0.2305 eV/NN and 0.0035 eV/NNN.<sup>9</sup> In order to compare directly with experimental observations, results are presented for one monolayer (ML) of Co deposited at 1.5 ML/min (1 ML= $1.53 \times 10^{15}$  atoms/cm<sup>2</sup>) with the substrate held at 275 K. The film was subsequently annealed to 350 K for 30 seconds.

Experimental results were obtained from Co growth on bulk single crystal Cu(100) samples.<sup>8</sup> Cu substrates were cleaned by repeated Ar<sup>+</sup> ion sputter and anneal (600 C) cycles. Co was grown by electron-beam evaporation at pressures  $<5 \times 10^{-10}$  mbar. Samples were transferred *in-situ* into an ultrahigh vacuum scanning transmission electron microscope (STEM) for nanometer resolution secondary electron imaging.<sup>13</sup>

In Fig. 1 examples of high resolution UHV secondary electron micrographs of the first (a) and second (b) growth modes are shown. The  $\langle 100 \rangle$  direction is denoted by the inserted arrow. Gray scale images have been rendered as 3 dimensional (3-D) for comparison with later simulation results. Both films consist of 0.2 ML of Co grown at 300 K on Cu(100) at 0.15 ML/min. Because the restructuring is observed for such small amounts of deposit (Fig. 1(b)), we believe that the relief of strain in the Co film is not a significant driving force in the early stages of growth. Restructuring takes the form of facets with low energy  $\langle 110 \rangle$  steps, suggesting that the lowering of free energy is the driving force. The large scale faceting and step edge restructuring shown in Fig. 1(b) was not well reproduced by kinetic Monte Carlo simulations in the presence of single atom high steps<sup>9</sup>, although when annealed simulated structures exhibit morphologies remarkably similar to those produced during growth experiments. Experimental and computed morphologies for growth near step bands are rendered as 3-D in Fig. 2. Brighter areas are higher. Simulations are in the left column (Fig. 2(a, c)) and SEM results at right (Fig. 2(b, d)). White arrows inserted into the images denote the  $\langle 100 \rangle$  direction. The simulations include 1.0 ML of Co grown near step bands aligned along  $\langle 100 \rangle$  (Fig. 2(a)) and  $\langle 110 \rangle$  (Fig. 2(c)) followed by a 30 second anneal at 350 K. No differentiation is made between Co and Cu atoms. The SEM results also include growths of 1.0 ML with step bands aligned close to  $\langle 100 \rangle$  (Fig. 2(b)) and  $\langle 110 \rangle$  (Fig. 2(d)), however, without annealing.

The simulation results (Fig. 2(a, c)) contain large rectangular vacancies from which Cu has migrated. Before annealing these were exposed regions of the Cu substrate. The experimental results (Fig. 2(b, d)) contain similar features, although the length scales are about two times larger. Adjacent to the  $\langle 100 \rangle$  step bands in Fig. 2(a) are long connected vacancy regions with  $\langle 110 \rangle$  facets separated from the step bands by Co islands (see e.g. region around the arrow). These regions are within the adatom random walk distance of the step band. The Co island density during growth was low in this region, leaving exposed Cu after the growth. This Cu was then free to migrate during the anneal. Co which migrated over the step from this denuded region formed islands at the step bands. Regions of similar morphology can be seen in our SEM data along  $\langle 100 \rangle$  step bands. Such a region surrounds the arrow in Fig. 2(b). The large rectangular vacancies in the simulation terraces were formed by incomplete Co coverage, from which Cu migrated during annealing. Similar structures were also observed in the SEM data, as can be seen in the terrace of Fig. 2(d). Inclusions into the  $\langle 110 \rangle$  step bands (Fig. 2(c, d)) are more rectangular than those into  $\langle 100 \rangle$  step bands, and are not separated from the step band by Co islands.

The top level atomic species for the simulations before (left) and after (right) annealing are shown in Fig. 3 for  $\langle 100 \rangle$  (top) and  $\langle 110 \rangle$  (bottom) step bands. Black squares are Co atoms and white squares are Cu atoms. Figure 3(b, d) are the same simulation results as shown in Fig. 2(a, c). Cu has clearly migrated from exposed areas to cover and or surround the Co islands. Very few Co islands are exposed (on top) after the anneal, however, a large number of Co atoms along steps are exposed. The shapes of Co islands are now much less rectangular and closer to those obtained experimentally from the first growth mode. These islands are now surrounded by Cu (i.e. part of a terrace). Interdiffusion has obviously increased dramatically during annealing.

We believe the activation energies for processes at steps are lower than our model predicts, which caused the discrepancy between the simulations of RT growth and the experimental morphologies. Transition rates in our model are dependent on attempt frequency, temperature, and the parameters A and B. A change in any of these parameters will change the rate at which processes occur. Increasing T, as in our annealing simulations, is equivalent to increasing  $R_0$ , or decreasing  $\epsilon$ . These parameters, then, have meaning only as they compare to each other. The exposed Cu atoms are apparently close to an activation energy threshold since a small increase in temperature (75 K) dramatically increases their mobility. One possible method to improve the simulations is to change the model for activation energy ( $\epsilon$ ). Lowering  $\epsilon$  for processes whose beginning bond energies are smaller should increase the rate of processes for atoms with lower coordination, such as at steps. We have chosen not to search the vast parameter space for combinations which produce the experimentally observed morphology. Rather, we have approximated the increased mobility of Cu atoms at defects by annealing. This produced morphologies remarkably similar to those observed in SEM data.

SEM results not shown reveal a continuum of combinations of the first and second growth modes. We cannot correlate contamination levels with growth mode, although a surfactant-like effect of some contaminant cannot be ruled out. We believe this diversity is instead due to variations in defect densities. The width and density of step bands was not constant between different samples used for the growth experiments. Agglomerations of vacancies were evident in some samples, suggesting a high density of defects we could not detect. Samples with higher defect densities would exhibit an increased proportion of the second growth mode. Differences in defect density and the resultant changes in activation energies, then, would account for the differences in observed morphology. Lowered activation energies for Cu

atoms could be the result of relaxation near defects, or changes in the strain field caused by nearby Co atoms.

### **Aknowledgements**

The authors would like to thank Dr. G. G. Hembree for collaboration in the experimental work. This work is supported by ONR under grant No. N00014-93-1-0099.

## References

- 1 F. Thibaudau and J. Cousty, *Ultramicroscopy* **42-44**, 511 (1991).
- 2 M. Giesen, *et al.*, *J. Vac. Sci Technol. A* **10**, 2597 (1992).
- 3 P. Stoltze, *J. Phys. Condens. Matter* **6**, 9495 (1994).
- 4 Z.-J. Tian and T. S. Rahman, *Phys. Rev. B* **47**, 9751 (1993).
- 5 M. Klaua, *et al.*, *Surf. Sci.* **381**, 106 (1997).
- 6 A. K. Schmid, *et al.*, *Phys. Rev. B* **48**, 2855 (1993).
- 7 M. Giesen, F. Schmitz, and H. Ibach, *Surf. Sci.* **336**, 269 (1995).
- 8 S. T. Coyle, G. G. Hembree, and M. R. Scheinfein, *J. Vac. Sci. Technol. A* **15**, 1785 (1997).
- 9 S. T. Coyle, J. L. Blue, and M. R. Scheinfein, *J. Vac. Sci. Technol.* (submitted).
- 10 J. L. Blue, to be published .
- 11 M. T. Kief and W. F. Egelhoff, Jr., *Phys. Rev. B* **47**, 10785 (1992).
- 12 L. Z. Mezey and J. Giber, *Jpn. J. Appl. Phys.* **21**, 1569 (1982).
- 13 K. R. Heim, *et al.*, *J. Appl. Phys.* **74**, 7422 (1993).



## Figure Captions

FIG. 1. Secondary electron micrographs of 0.2 ML Co/Cu(100) grown at 300 K, which show examples of the first (a) and the second (b) growth modes described in the text. White arrows denote the  $\langle 100 \rangle$  direction. Gray scale images have been rendered as 3-D.

FIG. 2. Simulation results (a, c) and SEM results (b, d) for 1 ML Co/Cu(100) grown at RT near  $\langle 100 \rangle$  (a, b) and  $\langle 110 \rangle$  (c, d) step bands. The simulations were annealed at 350 K for 30 seconds. Bright regions are higher. White arrows denote the  $\langle 100 \rangle$  direction. Gray scale images have been rendered as 3-D.

FIG. 3. Simulation results for 1 ML Co/Cu(100) before (a, c) and after (b, d) annealing. The atomic species of the topmost exposed atom is shown. Black squares are Co atoms and white squares are Cu atoms.

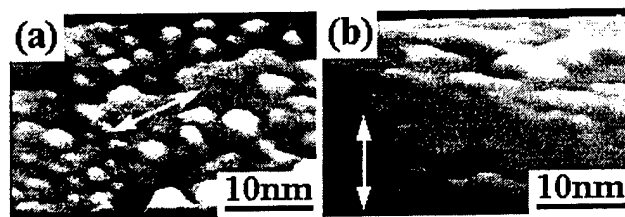


FIG. 1

Coyle, et al.

APL

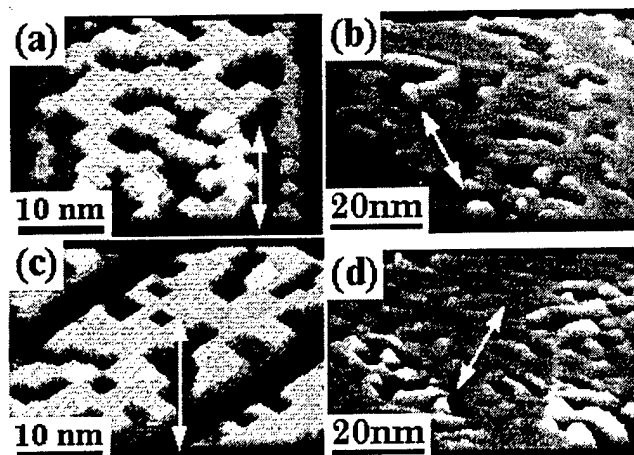


FIG. 2

Coyle et al

APL

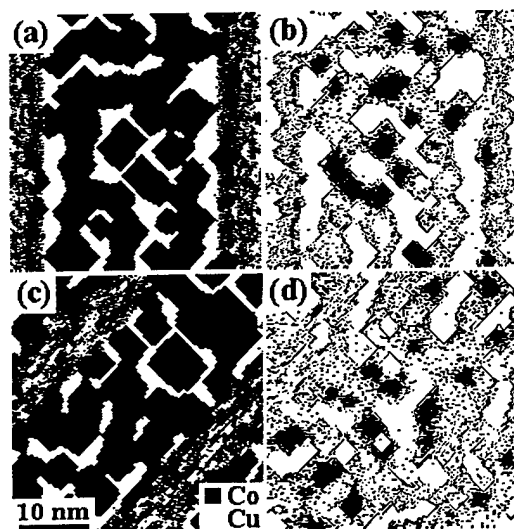


FIG. 3

Coyle et al

APL